FREQUENCY-DEPENDENT RECONSTRUCTION OF IMBALANCES[*]

JENNY NIEBSCH[†] AND RONNY RAMLAU[‡]

Abstract. Imbalances in rotating machines cause vibrations of the system and may lead to an early wearout of the machine. In this paper, we consider the development of an algorithm for the detection (and subsequent correction) of imbalances from vibrational measurements at certain nodes of the system. Since, e.g., modern wind turbines operate with variable speed, the vibration data are usually collected during changing rotational speed. Based on a mathematical model that connects the measured vibrations at different rotational speeds with the imbalance distribution, we propose an algorithm for its reconstruction. The reconstruction algorithm is based on a tensor product formulation of the forward model. Test examples with artificial data are used to verify our approach.

Key words. integral equation, Kronecker product, inverse problem, tensor product, regularization

AMS subject classifications. 65N21, 47A52, 15A05

1. Introduction. Imbalances affect all types of rotating machinery, e.g., generators, aircraft engines, or wind turbines [8, 30]. Mathematically, an imbalance is described as an additional mass m located at a distance r from the center of rotation and at an angle φ to a prior chosen zero mark, i.e., $p^0 = mre^{i\varphi}$. During the operation of the machinery with a certain frequency, imbalances induce forces that cause displacements in the form of vibrations of the machine. These vibrations are of the same frequency as the rotating frequency. Sometimes vibrations can be measured by mounting sensors at certain positions, e.g., at the casing of an aircraft engine or in the nacelle of a wind turbine. The identification of an imbalance from measurements allows to eliminate or at least reduce it by placing an appropriate counterweight opposite to the determined position of the eccentric mass. A safe and economic operation of a rotating machinery very much depends on a well-balanced state. Therefore the reconstruction of imbalances from vibration measurements is an important topic.

The mathematical description of the connection between the load from an imbalance and the displacement involves a partial differential equation (PDE) which is seldom explicitly solvable. Applying a finite element method, the PDE can be transformed into a system of ordinary differential equations (ODEs) of second order; cf. [6]:

$$(1.1) \qquad (L\mathbf{u})(t) := \mathbf{M}\mathbf{u}''(t) + \mathbf{D}\mathbf{u}'(t) + \mathbf{S}\mathbf{u}(t) = \mathbf{p}(t).$$

The chosen number of nodes in the finite element model and the number of degrees of freedom (DOF) of each node determine the size $N =$ Number of nodes $\times$ Number of DOF of the vector of displacements $\mathbf{u}$ and the vector of loads $\mathbf{p}$. Accordingly, the mass matrix $\mathbf{M}$, the damping matrix $\mathbf{D}$, and the stiffness matrix $\mathbf{S}$ are square matrices of dimension $N \times N$. Depending on the direction of the force and the possible location of the imbalance, the forces only affect certain DOF. In most applications there are only a few nodes where imbalances and resulting forces can occur. Hence, the vector $\mathbf{p}$ is usually sparse.

Unfortunately, equation (1.1) cannot be used directly to compute $\mathbf{p}$ from measured displacement data $\mathbf{u}$. Since the data are usually corrupted by noise and the operator L as a differential operator can not be stably evaluated, other methods for finding $\mathbf{p}$ and with it

---

[†]Johann Radon Institute for Computational and Applied Mathematics, Altenbergerstraße 69, 4040 Linz, Austria (jenny.niebsch@oeaw.ac.at).

[‡]Industrial Mathematics Institute, Johannes Kepler University Linz, Altenbergerstraße 69, 4040 Linz, Austria (ronny.ramlau@jku.at).

the imbalance have to be employed. The transformation of (1.1) into an equivalent operator equation of the form

$$(1.2) \qquad\qquad (T\mathbf{p})(t) = \mathbf{u}(t)$$

allows us to treat the problem as an ill-posed inverse problem and solve it by regularization techniques.

In case the rotating frequency f or the angular velocity $\omega = 2\pi f$ is constant or quasi-static, the transformation from (1.1) into (1.2) is simple. Using the fact that the load induced by an imbalance at the k-th DOF, $p_k^0 = m_k r_k e^{i\varphi_k}$, is a harmonic centrifugal force computed by $p_k(t) = p_k^0 \omega^2 e^{i\omega t}$, (1.2) reduces to a system of algebraic equations. With $\mathbf{p}^0 = (p_1^0, \ldots, p_N^0)^T$, the vector $\mathbf{p}(t)$ of the load functions for all DOF is given by

$$\mathbf{p}(t) = \mathbf{p}^0 \cdot \omega^2 e^{i\omega t}.$$

Assuming $\mathbf{u}(t) = \mathbf{u}^0 e^{i\omega t}$ and inserting it into the ODE system (1.1), we get an algebraic system for the amplitude vector $\mathbf{u}^0$ and the imbalance vector $\mathbf{p}^0$,

$$(1.3) \qquad\qquad \mathbf{T}\mathbf{p}^0 := \left(-\mathbf{M} + \frac{i}{\omega}\mathbf{D} + \frac{1}{\omega^2}\mathbf{S} \right)^{-1} \mathbf{p}^0 = \mathbf{u}^0.$$

It can be reduced in dimension by taking into account the sparse structure of $\mathbf{p}^0$ and the fact that $\mathbf{u}^0$ can usually only be measured at a few DOF. This case was solved earlier and applied to several industrial applications; see, e.g., [3, 24, 25].

However, practical applications often require the measurement of the displacement while ω is not constant. For instance, wind turbines operate with variable speed. Another example is a test run of an aircraft engine which is so expensive that it saves a lot of money to take measurements during an idle to maximum cycle or vice versa. Thus, the investigation of the imbalance reconstruction problem with time-dependent ω is well justified.

The transformation of (1.1) into (1.2) is mathematically difficult as a time-dependent ω changes the load from an imbalance with the simple structure $\mathbf{p}(t) = \mathbf{p}^0 \omega^2 e^{i\omega t}$ (allowing the simplifications mentioned above) to

$$(1.4) \quad \begin{aligned} \mathbf{p}(t) &= \Re(\mathbf{p^0}[\omega^2(t) - i\omega'(t)]e^{i\,\varphi(t)}) \\ &= \left(m_k r_k \omega^2(t)\cos(\varphi(t) + \varphi_k) + m_k r_k \omega'(t)\sin(\varphi(t) + \varphi_k) \right)_{k=1}^N, \end{aligned}$$

with $\varphi'(t) = \omega(t)$. The transformation problem for this case was considered in [26]. Because standard methods like the transformation into a system of first-order ODEs or the use of numerical ODE solvers were found to be unsuitable, equation (1.1) with a general time-dependent function $\mathbf{p}(t)$ as right-hand side and without the damping term $\mathbf{D}\mathbf{u}'(t)$ was transformed into an equivalent integral equation representing (1.2). Moreover, tensor products of function spaces and operators were used to represent this integral equation in an efficient way and to simplify the discretization process. In this way the direct problem of computing the displacements $\mathbf{u}(t)$ for a given load function $\mathbf{p}(t)$ was solved and resulted in a description of the operator T in (1.2).

As mentioned above, the inverse problem of reconstructing $\mathbf{p}(t)$, or in our applications $\mathbf{p}^0$ in (1.4), from measured data $\mathbf{u}(t)$ is ill-posed. Its solution is the topic of this paper. In Section 2 we present the tensor notation of the operator T derived in [26]. In Section 3 we include all restrictions arising in our application into the mathematical formulation. This leads to a slightly different formulation of the operator T from (1.2), i.e., now we consider T as an operator acting on $\mathbf{p}^0$ instead of $\mathbf{p}(t)$. T is again represented in terms of tensor products. In Section 4

we briefly summarize the options to solve the ill-posed inverse problem of reconstructing the imbalance $\mathbf{p}^0$ from given noisy data $\mathbf{u}$. Section 5 is devoted to the discretization of the problem using a Galerkin scheme. The discretized operator can be represented using Kronecker products. Finally, Section 6 states the final algorithm for the reconstruction of an imbalance distribution from given data and provides numerical test examples to verify the new reconstruction algorithm.

2. Integral formulation of the general forward problem. In [26] a formulation in the form (1.2) was presented for the case of a machine without damping or with negligible damping and a time-dependent load vector $\mathbf{p}(t)$ as well as unknown initial conditions. The ODE system then reads:

$$(2.1) \quad \mathbf{M}\mathbf{u}''(t) + \mathbf{S}\mathbf{u}(t) = \mathbf{p}(t), \quad \mathbf{u}(0) = \alpha, \ \mathbf{u}'(0) = \beta, \qquad \alpha, \beta \in \mathbb{R}^N, \ t \in [0, T_e],$$

with

$$\mathbf{p}(t) = (p_1(t), \ldots, p_N(t))^T, \quad \mathbf{u}(t) = (u_1(t), \ldots, u_N(t))^T \quad \in (L_2([0, T_e]))^N.$$

The space $(L_2([0, T_e]))^N$ can be represented as the tensor product $\mathbb{R}^N \otimes L_2([0, T_e])$. For details we refer to [26, Section 3]. The representation of $\mathbf{p}(t)$ and $\mathbf{u}(t)$ as tensor products is expressed as

$$\mathbf{p}(t) = \sum_{i=1}^N \mathbf{e}_i \otimes p_i(t)$$

and for $\mathbf{u}(t)$ likewise.

To present the solution operator T of (2.1), we define the compact integral operator $K : L_2[0, T_e] \to L_2[0, T_e]$ by

$$(Kp_i)(t) := \int_0^t (t - \theta)p_i(\theta)d\theta,$$

and the linear operators which are represented by the matrices

$$(2.2) \qquad\qquad\qquad \mathbf{B} := \mathbf{M}^{-1} \quad \text{and} \quad \mathbf{C} := \mathbf{M}^{-1}\mathbf{S}.$$

The operator $\mathcal{K} : \mathbb{R}^N \otimes L_2([0, T_e]) \times \mathbb{R}^N \times \mathbb{R}^N \to \mathbb{R}^N \otimes L_2([0, T_e])$ is defined by

$$(\mathcal{K}[\mathbf{p}, \ \alpha, \ \beta])(t) = (\mathbf{B} \otimes K) \left(\sum_{i=1}^N \mathbf{e}_i \otimes p_i(t) \right) + \sum_{i=1}^N \alpha_i \mathbf{e}_i \otimes 1 + \sum_{i=1}^N \beta_i \mathbf{e}_i \otimes t,$$

where $\mathbf{B} \otimes K$ is the tensor product of $\mathbf{B}$ and K, $(\mathbf{e}_i)_{i=1}^N$ is the orthonormal basis of $\mathbb{R}^N$, and 1 denotes the constant function $f(t) = 1$ on $L_2([0, T_e])$. The operator $\mathcal{A}$ and the identity $\mathbf{I}$ are defined by

$$\mathcal{A} : \mathbb{R}^N \otimes L_2([0, T_e]) \to \mathbb{R}^N \otimes L_2([0, T_e]) \qquad \mathbf{I} : \mathbb{R}^N \otimes L_2([0, T_e]) \to \mathbb{R}^N \otimes L_2([0, T_e])$$
$$\mathcal{A} = \mathbf{C} \otimes (-K), \qquad\qquad\qquad\qquad \mathbf{I} = \mathbf{I}_{\mathbb{R}^N} \otimes \mathbf{I}_{L_2};$$

see [26, (3.3) and Cor. 3.8]. Here $\mathbf{I}_{\mathbb{R}^N}$ and $\mathbf{I}_{L_2}$ are the identity operators in $\mathbb{R}^N$ and $L_2([0, T_e])$, respectively. With these preparations we can now present the equivalent integral representation of (2.1) as

$$(2.3) \qquad\qquad (T[\mathbf{p}, \ \alpha, \ \beta])(t) = ((\mathbf{I} - \mathcal{A})^{-1}\mathcal{K}[\mathbf{p}, \ \alpha, \ \beta])(t) = \mathbf{u}(t)$$

with

$$T : \mathbb{R}^N \otimes L_2([0, T_e]) \times \mathbb{R}^N \times \mathbb{R}^N \to \mathbb{R}^N \otimes L_2([0, T_e]).$$

Equation (2.3) is discretized by a Galerkin scheme, which results in a representation in terms of Kronecker products. The forward computation was implemented, and test examples presented in [26] show the stability of the method.

3. Computing the imbalance distribution from vibration measurements—the inverse problem. Now that our problem is represented in the form (2.3), we can attempt to solve the inverse problem where $\mathbf{u}(t)$ is given and $[\mathbf{p}(t), \alpha, \beta]$ is to be determined. Considering the application we have in mind, several restrictions and constraints have to be taken into account. First of all, the vibrations $\mathbf{u}$ can only be measured for certain DOF, e.g., for the radial displacements, and at certain positions where sensors can be placed, e.g., in the nacelle of a wind turbine. Additionally, its measurements are taken at discrete times. Secondly, the sparse structure of the imbalance vector $\mathbf{p}^0$ can be used. However, most important is the third fact, namely that we are not really interested in $\mathbf{p}(t)$ as a function of t (cf. (1.4)). Assuming we know the time-dependent angular velocity $\omega(t)$ from measurements at certain points in time, we are only interested in recovering $\mathbf{p}^0$.

3.1. Measurement restrictions. Let N be the number of degrees of freedom in the rotating system. Then $\mathbf{u} = (u_i(t))_{i=1,\dots,N}$ is a vector of N L_2-functions, where each function $u_i(t)$ describes the displacement of the ith DOF. We assume that the displacement can only be measured at a number of s DOF indexed by $N_1, \dots, N_s$, $s \leq N$. We define $\mathbf{s} := \{N_1, \dots, N_s\} \subset \{1, \dots, N\}$ and the operator $P_\mathbf{s}$ as an orthogonal projection:

$$P_\mathbf{s} : \mathbb{R}^N \otimes L_2([0, T_e]) \longrightarrow \mathbb{R}^s \otimes L_2([0, T_e])$$

(3.1)
$$\mathbf{u} = \sum_{i=1}^N \mathbf{e}_i \otimes u_i \mapsto \sum_{i=1}^s \mathbf{e}_i \otimes u_{N_i} =: \mathbf{u_s}.$$

Using tensor product notation, we have

$$P_\mathbf{s} = \mathbf{I_s} \otimes \mathbf{I}_{L_2}$$

with the identity operator $\mathbf{I}_{L_2}$ of $L_2([0, T_e])$ and the $(s \times N)$-matrix $\mathbf{I_s}$ with the entries

(3.2)
$$(\mathbf{I_s})_{ij} = \begin{cases} 1 & \text{if } j = N_i, \\ 0 & \text{otherwise.} \end{cases}$$

Applying $P_\mathbf{s}$ on both sides of (2.3), we arrive at

$$(P_\mathbf{s}(\mathbf{I} - \mathcal{A})^{-1} \mathcal{K} [\mathbf{p}, \alpha, \beta])(t) = \mathbf{u_s}(t).$$

3.2. Restriction to imbalance positions. From the N DOF in our system, let only r be subjected to a load from an imbalance. Let $\{L_1, \dots, L_r\} \subset \{1, \dots, N\}$ be the set of indices of the DOF that are subjected to imbalances. We define the restrictions

(3.3)
$$\bar{\mathbf{p}} := \sum_{i=1}^r \mathbf{e}_i \otimes p_{L_i}, \qquad \bar{\mathbf{B}} := (\mathbf{B}_{L_1}, \dots, \mathbf{B}_{L_r}) \in \mathbb{R}^{N \times r},$$

where $\mathbf{B}_{L_i}$, $i = 1, \ldots, r$, is the L_i-th column of the matrix $\mathbf{B}$ and $\mathbf{e}_i$, $i = 1, \ldots, r$, are the unit vectors in $\mathbb{R}^r$. Then we define the operator $\bar{\mathcal{K}}$ as

$$(3.4) \qquad \bar{\mathcal{K}}[\bar{\mathbf{p}}, \ \alpha, \ \beta] = (\bar{\mathbf{B}} \otimes K) \left(\sum_{i=1}^{r} \mathbf{e}_i \otimes p_{L_i} \right) + \sum_{i=1}^{N} \alpha_i \mathbf{e}_i \otimes 1 + \sum_{i=1}^{N} \beta_i \mathbf{e}_i \otimes t.$$

Now the problem for the restricted imbalance and data situation reads as

$$(3.5) \qquad (P_{\mathbf{s}}(\mathbf{I} - \mathcal{A})^{-1} \bar{\mathcal{K}} \, [\bar{\mathbf{p}}, \ \alpha, \ \beta])(t) = \mathbf{u}_{\mathbf{s}}(t).$$

3.3. Reconstruction of the imbalance vector $\mathbf{p}^0$. The aim of all our considerations is the reconstruction of the imbalance vector $\bar{\mathbf{p}}^0$ which is hidden in the load vector

$$\bar{\mathbf{p}}(t) = \Re[\bar{\mathbf{p}}^0(\omega^2(t) - i\omega'(t))e^{i\varphi(t)}].$$

The solution of the inverse problem (3.5) for given $\mathbf{u}_{\mathbf{s}}$ would provide us with an approximate solution for $\bar{\mathbf{p}}(t)$. The angular velocity $\omega(t)$ as well as the angle $\varphi(t)$ can be measured along with $\mathbf{u}_{\mathbf{s}}$. The remaining question is how to determine $\bar{\mathbf{p}}^0$.

By a splitting into real and imaginary part, $\bar{\mathbf{p}}^0 = \bar{\mathbf{p}}^R + i\bar{\mathbf{p}}^I$, and the definition

$$(3.6) \qquad \Omega(t) := (\omega^2(t) - i\omega'(t))e^{i\varphi(t)} = \Omega^R(t) + i\Omega^I(t)k,$$

we can write $\bar{\mathbf{p}}(t)$ as

$$\bar{\mathbf{p}}(t) = \bar{\mathbf{p}}^R \Omega^R(t) - \bar{\mathbf{p}}^I \Omega^I(t).$$

We assume that $\omega(t)$, which is given only at discrete times, can be approximated sufficiently accurately by a C^1-function and thus $\Omega(t)$ can be determined. Then we use the special structure of $\bar{\mathbf{p}}(t)$ when applying $\bar{\mathcal{K}}$ from (3.4): we have

$$
\begin{aligned}
(3.7) \qquad (\bar{\mathbf{B}} \otimes K) \left(\sum_{i=1}^{r} \mathbf{e}_i \otimes \bar{p}_{L_i} \right) &= \sum_{i=1}^{r} \bar{\mathbf{B}} \mathbf{e}_i \otimes K \bar{p}_{L_i} \\
&= \sum_{i=1}^{r} \bar{\mathbf{B}} \mathbf{e}_i \otimes [\bar{p}_{L_i}^R (K\Omega^R)(t) - \bar{p}_{L_i}^I (K\Omega^I)(t)] \\
&= \sum_{i=1}^{r} \bar{\mathbf{B}} \mathbf{e}_i \otimes [K\Omega^R, -K\Omega^I] \begin{bmatrix} \bar{p}_{L_i}^R \\ \bar{p}_{L_i}^I \end{bmatrix} \\
&= (\bar{\mathbf{B}} \otimes K) \sum_{i=1}^{r} \mathbf{e}_i \otimes [\Omega^R, -\Omega^I] \begin{bmatrix} \bar{p}_{L_i}^R \\ \bar{p}_{L_i}^I \end{bmatrix}.
\end{aligned}
$$

With the definition

$$
\begin{aligned}
(3.8) \qquad \mathcal{K}_\Omega \left[\sum_{i=1}^{r} \mathbf{e}_i \otimes \begin{bmatrix} \bar{p}_{L_i}^R \\ \bar{p}_{L_i}^I \end{bmatrix}, \alpha, \beta \right] &:= (\bar{\mathbf{B}} \otimes K) \sum_{i=1}^{r} \mathbf{e}_i \otimes [\Omega^R, -\Omega^I] \begin{bmatrix} \bar{p}_{L_i}^R \\ \bar{p}_{L_i}^I \end{bmatrix} \\
&\quad + \sum_{i=1}^{N} \alpha_i \mathbf{e}_i \otimes 1 + \sum_{i=1}^{N} \beta_i \mathbf{e}_i \otimes t,
\end{aligned}
$$

we get a new formulation of (3.5):

$$(3.9) \qquad (P_{\mathbf{s}}(\mathbf{I} - \mathcal{A})^{-1} \mathcal{K}_\Omega) \left[\sum_{i=1}^{r} \mathbf{e}_i \otimes \begin{bmatrix} \bar{p}_{L_i}^R \\ \bar{p}_{L_i}^I \end{bmatrix}, \ \alpha, \ \beta \right] = \mathbf{u}_{\mathbf{s}}.$$

Following this approach and using the abbreviations

$$(3.10) \qquad T := P_{\mathbf{s}}(\mathbf{I} - \mathcal{A})^{-1}\mathcal{K}_{\Omega}, \qquad x := \left[\sum_{i=1}^{r} \mathbf{e}_i \otimes \begin{bmatrix} \bar{p}_{L_i}^R \\ \bar{p}_{L_i}^I \end{bmatrix}, \alpha, \beta \right], \qquad y := \mathbf{u}^{\mathbf{s}},$$

we state our inverse problem as:

$$Tx = y,$$

where T is now an operator between $X = \mathbb{R}^{2(r+N)}$ and $Y = \mathbb{R}^s \otimes L_2[0, T_e]$, and x is to be reconstructed from given noisy data y^δ with $\|y - y^\delta\| \leq \delta$. We remark that x is not a vector of functions of t anymore but the vector of imbalance values and initial values. We also recall that we are interested in the imbalance values $\bar{p}_{L_i}^R, \bar{p}_{L_i}^I, i = 1, \ldots, r$, only.

4. Regularization. Inverting T involves the inversion of the compact integral operator $\mathcal{K}$, and the problem is thus ill-posed, i.e., it requires regularization techniques for its solution. Applying regularization basically means that the generalized inverse $T^\dagger$ of T is replaced by a family of continuous operators $R_\gamma, \gamma \in \mathbb{R}^+$, that converges pointwise to the generalized inverse. The regularization parameter γ has to be adapted to the amount of noise in the data. For a review on the theory of inverse problems, we refer to the monographs [4, 5, 15, 19, 22, 23, 29]. Frequently used regularizations are the following:

- Truncated singular value decomposition (SVD) is based on the representation of the generalized inverse of T using the singular system $\{v_n, u_n; \sigma_n\}$ of T,

$$T^\dagger y = \sum_{n=1}^{\infty} \sigma_n^{-1}\langle y, u_n \rangle v_n.$$

  The method, applied to noisy data y^δ fulfilling $\|y - y^\delta\| \leq \delta$, is defined as

$$R_\gamma y = \sum_{\sigma_n > \gamma} \sigma_n^{-1}\langle y, u_n \rangle v_n,$$

  where the regularization parameter γ acts as a lower threshold for the singular values. The method has been used in particular for the solution of discrete ill-posed problems [10] and in combination with the L-curve method [11, 12, 13] for the determination of the cut-off.

- Tikhonov regularization [27, 28] is probably the best-analyzed regularization method. Here the regularization operator R_γ applied to noisy data y^δ is given by

$$x_\gamma^\delta = R_\gamma y^\delta = (T^*T + \gamma I)^{-1}T^*y^\delta.$$

  For an analysis of the method with a linear operator we refer in particular to [4, 7]. The regularization parameter γ has to be chosen appropriately, e.g., according to Morozov's discrepancy principle [23], where γ is chosen such that the residual is of the same magnitude as the noise level, i.e., $\|Tx_\gamma^\delta - y^\delta\| \leq C\delta$. Alternatively, heuristic parameter choice rules that determine the regularization parameter independently of the noise level can be used; see, e.g., [16, 17, 18] and the references therein.

- Iterative methods aim at finding an approximate solution by minimizing the residual $\|y^\delta - Ax\|$ or, equivalently, by finding an approximate solution of the normal equation

$$T^*Tx = T^*y^\delta.$$

  Regularization is obtained by an early termination of the iteration, e.g., based on the discrepancy principle. Examples are Landweber iteration [2, 20] or the conjugate gradient method [1, 9, 14, 21].

Since Tikhonov regularization as well as the iterative methods require the frequent application of T and T^*, which requires in particular the evaluation of $(\mathbf{I} - \mathcal{A})^{-1}$ and $(\mathbf{I} - \mathcal{A}^*)^{-1}$, we opted for the use of the truncated SVD. Note that the computation of the singular system of the discretized operator T is not too expensive since the operator is restricted to the few imbalance and measurement positions resulting in a low-dimensional matrix.

5. Discretization. For the discretization of (3.9), we take advantage of the tensor representation. It was shown in [26] that we only need to discretize the function space $L_2[0, T_e]$ and use the canonical Euclidean basis in $\mathbb{R}^s, \mathbb{R}^N$, and $\mathbb{R}^r$, denoted by $\{\mathbf{e}_i\}_{i=1}^{s,N,r}$.

5.1. Discretization of $L_2[0, T_e]$. Consider the n-dimensional subspace $L_{2,n}[0, T_e] \subset L_2[0, T_e]$ determined by a basis $\{\psi_1, \ldots, \psi_n\}$, e.g., the normed hat functions. An L_2-function f can be projected onto $L_{2,n}$ by

$$P_n f = f_n(t) = \sum_{j=1}^{n} f_j \psi_j(t), \qquad t \in [0, T_e],$$

where the coefficient vector $(f_j)_{j=1}^n$ is given by

$$(f_j)_{j=1}^n = \mathbf{D}^{-1} \underline{\mathbf{f}}, \qquad \text{with} \quad \underline{\mathbf{f}} = (\langle \psi_j, f \rangle)_{j=1}^n \quad \text{and} \quad \mathbf{D} = (\langle \psi_i, \psi_j \rangle)_{i,j=1}^n.$$

Whenever the basis functions are orthonormal, which is not the case for hat functions, the matrix $\mathbf{D}$ becomes the identity matrix in $\mathbb{R}^n$. In this way the functions $\Omega_R(t), \Omega_I(t)$, the functions $f(t) = 1$ and $f(t) = t$, and the components $u_{N_i}(t), i = 1, \ldots, s$, of the data $y \in \mathbb{R}^s \otimes L_2[0, T_e]$ can be projected onto the subspace $L_{2,n}$. In particular, we have that $u_{N_i}(t) = \sum_{j=1}^{n} u_{N_i}^j \psi_j(t)$. The discretized data vector can be written in *Kronecker product* notation as

$$(5.1) \qquad y \approx \mathbf{y}_n = \sum_{i=1}^{s} \mathbf{e}_i \otimes (u_{N_i}^j)_{j=1}^n.$$

We remark that the number of entries of $\mathbf{y}_n$ is $s \cdot n$.

5.2. Discretization of T. We present the discretized version of T based on a Galerkin formulation. It was shown in [26] that the Galerkin method applied to tensor products leads to Kronecker products of matrices. This was in fact a major motivation to use the tensor product formulation in the first place.

We use the following definitions:

$$(5.2) \qquad \mathbf{F} = (\langle \psi_i, K \psi_j \rangle)_{i,j=1,\ldots,n},$$

$$(5.3) \qquad \mathbf{\Omega} = \begin{bmatrix} \Omega_1^R & -\Omega_1^I \\ \vdots & \vdots \\ \Omega_n^R & -\Omega_n^I \end{bmatrix},$$

$$(5.4) \qquad \underline{\mathbf{c}} = (\langle \psi_j, 1 \rangle)_{j=1}^n \quad \text{and} \quad \underline{\mathbf{d}} = (\langle \psi_j, t \rangle)_{j=1}^n.$$

Recall that $(\Omega_j^{R,I})_{j=1}^n = \mathbf{D}^{-1} \left(\langle \psi_j, \Omega^{R,I} \rangle \right)_{j=1}^n$.

It is shown without difficulty (see Appendix A) that when using a Galerkin scheme, the discretized form of

$$(5.5) \qquad \sum_{i=1}^{N} \mathbf{e}_i \otimes z_i(t) = \mathcal{K}_\Omega \left[\sum_{i=1}^{r} \mathbf{e}_i \otimes \begin{bmatrix} \bar{p}_{L_i}^R \\ \bar{p}_{L_i}^I \end{bmatrix}, \alpha, \beta \right]$$

is given in terms of Kronecker products by

$$(5.6) \qquad \sum_{i=1}^{N} \mathbf{e}_i \otimes \mathbf{z}_i = [(\bar{\mathbf{B}} \otimes \mathbf{F})(\mathbf{I}_{\mathbb{R}^r} \otimes \mathbf{\Omega}), \mathbf{I}_{\mathbb{R}^N} \otimes \underline{\mathbf{c}}, \mathbf{I}_{\mathbb{R}^N} \otimes \underline{\mathbf{d}}] \begin{bmatrix} \sum_{i=1}^{r} \mathbf{e}_i \otimes \begin{bmatrix} \bar{p}_{L_i}^{R} \\ \bar{p}_{L_i}^{I} \end{bmatrix} \\ \alpha \\ \beta \end{bmatrix}$$

with $\bar{\mathbf{B}}$ defined in (2.2) and (3.3), $\mathbf{F}$ from (5.2), $\mathbf{I}_{\mathbb{R}^r}, \mathbf{I}_{\mathbb{R}^N}$ the unit matrix on $\mathbb{R}^r$ and $\mathbb{R}^N$, $\mathbf{\Omega}$ from (5.3), and $\underline{\mathbf{c}}$ and $\underline{\mathbf{d}}$ from (5.4).

Again from [26], we know that $(\mathbf{I} - \mathcal{A})^{-1}$ applied to $\sum_{i=1}^{N} \mathbf{e}_i \otimes z_i(t)$ is discretized by the solution of the system

$$(5.7) \qquad \sum_{i=1}^{N} \mathbf{e}_i \otimes \mathbf{z}_i = [\mathbf{I}_{\mathbb{R}^N} \otimes \mathbf{D} - \mathbf{C} \otimes (-\mathbf{F})] \sum_{i=1}^{N} \mathbf{e}_i \otimes \mathbf{D}^{-1} \mathbf{u}_i.$$

Recall that $P_{\mathbf{s}}$ from (3.1) was the projection from $\mathbb{R}^N \otimes L_2$ onto $\mathbb{R}^s \otimes L_2$. Its projection $P_{n,\mathbf{s}}$ onto $\mathbb{R}^s \otimes L_{2,n}$ can be represented as the Kronecker product of the matrix $\mathbf{I}_s$ from (3.2) of dimension s and the matrix $\mathbf{D}$,

$$(5.8) \qquad P_{\mathbf{s},n} = \mathbf{I}_{\mathbf{s}} \otimes \mathbf{D}.$$

Combining (5.6), (5.7), and (5.8), the discretization of T from (3.10) is given by the matrix T_n with

$$(5.9) \quad T_n = (\mathbf{I}_{\mathbf{s}} \otimes \mathbf{I}_n)[\mathbf{I}_{\mathbb{R}^N} \otimes \mathbf{D} - \mathbf{C} \otimes (-\mathbf{F})]^{-1}[(\bar{\mathbf{B}} \otimes \mathbf{F})(\mathbf{I}_{\mathbb{R}^r} \otimes \mathbf{\Omega}), \mathbf{I}_{\mathbb{R}^N} \otimes \underline{\mathbf{c}}, \mathbf{I}_{\mathbb{R}^N} \otimes \underline{\mathbf{d}}].$$

Here the unit matrix $\mathbf{I}_n$ of dimension $n \times n$ appears as the product $\mathbf{D} \cdot \mathbf{D}^{-1}$. The inversion of the matrix $[\mathbf{I}_{\mathbb{R}^N} \otimes \mathbf{D} - \mathbf{C} \otimes (-\mathbf{F})]$ is difficult since the matrix is ill-conditioned. For our applications it turned out that just the smallest singular value of the matrix causes a difficulty. Therefore we have used a truncated singular value decomposition of that matrix by using the Matlab implemented function *pinv*. This stabilizes the problem sufficiently.

6. Algorithm and numerical examples. Algorithm 6.1 summarizes the steps necessary to compute the solution $\sum_{i=1}^{r} \mathbf{e}_i \otimes \begin{bmatrix} \bar{p}_{L_i}^{R} \\ \bar{p}_{L_i}^{I} \end{bmatrix}$ of the inverse problem for a given data vector $\mathbf{u}_s(t)$ and the frequency-related function $\Omega(t)$ from (3.6).

Algorithm 6.1: Algorithm for the solution of the inverse problem.

1: Given $T_e, n, \tau = \{t_1, \ldots, t_n\}$, and $\psi_j(t), u_{N_i}, j = 1, \ldots, n, \omega(\tau), \varphi(\tau)$.
2: Compute $\mathbf{B}, \mathbf{C}, \mathbf{D}, \mathbf{F}, \underline{\mathbf{c}}, \underline{\mathbf{d}}$, and $\mathbf{\Omega}$.
3: Compute $(u_{N_i}^{j})_{j=1}^{n} = \mathbf{D}^{-1} \left(\langle \psi_j, u_{N_i} \rangle \right)_{j=1}^{n}$, and write the discretized data y as in (5.1).
4: Compute T_n from (5.9).
5: Apply the truncated SVD to solve $T_n x = y$ with x as in (3.10).
6: Extract the imbalance $\bar{p}_{L_i}^{R}, \bar{p}_{L_i}^{I}$ from x as in (3.10), and compute the absolute value and angle of $\bar{p}_{L_i}^{R} + i\bar{p}_{L_i}^{I}$.
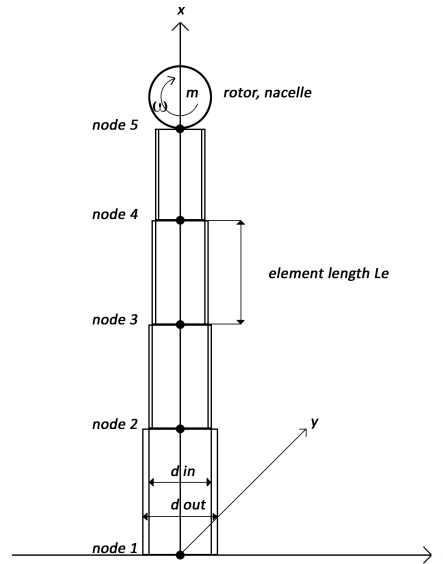

FIG. 6.1. *General finite element model of a wind turbine with 5 nodes.*

6.1. Numerical examples. To verify the algorithm we chose the system matrices $\mathbf{M}$ and $\mathbf{S}$ from the model of a wind turbine S77; cf. [25]. The simple structure of a wind turbine allows the use of models with few nodes. In this case the model has only 5 nodes; see Figure 6.1. Each node is considered having 2 degrees of freedom, i.e., the displacement in the radial direction z and the associated cross section slope. Hence, the matrices are of dimension $N \times N$ with $N = 10$. The matrices $\mathbf{B} = \mathbf{M}^{-1}$ and $\mathbf{C} = \mathbf{M}^{-1}\mathbf{S}$ are computed.

Looking for a rotor imbalance in a wind turbine rotor corresponds to finding an imbalance that only affects the displacement of the last node in the model in radial direction, i.e., the penultimate DOF. Thus, $\mathbf{p}_0$ can be restricted to $\bar{p}^0 = p_{N-1}^0$, and $\mathbf{B}$ is restricted accordingly. Sensors for vibration measurements are always placed in the nacelle of the turbine which is represented by the last node of the model as well as the rotor. Here the radial displacement is measured at a position corresponding again to the DOF $N - 1$. Normalized hat functions were chosen as a basis of $L_{2,n}([0, T])$. In this case, $\mathbf{D}$ can be computed explicitly as a tridiagonal $n \times n$ matrix. At this stage we have to rely on artificial data in all examples. Also we cannot yet specify the nature of the noise in the data. Hence, we just choose white Gaussian noise. The regularization parameter, i.e., the threshold for the singular values, has been fine-tuned experimentally.

6.1.1. Constant frequency. First we test the new algorithm for constant frequency. Thus, we can use the established technique (1.3) to produce the correct data. We define an imbalance $p_{N-1}^0 = 250 e^{i\pi/6}$ which corresponds to an imbalance of $250\,\mathrm{kg} \cdot \mathrm{m}$ at an angle of $30°$, i.e., blade 1 (angle $= 0°$) and blade 2 (angle $= 120°$) are imbalanced, and the imbalances sum up to p_{N-1}^0. We assume a constant frequency of 0.34 Hz, which is close to the first eigenfrequency of 0.354 Hz. Therefore $\omega_c = 0.68 \cdot \pi$ rad/s, $\varphi(t) = \omega_c t$, and $\Omega(t) = \omega_c^2 e^{i\omega_c t}$. As time interval we chose $[0, 5]$ s. It was divided into 500 subintervals of length $h = 0.01$ s, i.e., $n = 501$. We used the forward model for the constant frequency case, cf. (1.3), to compute the data $\mathbf{u}(t)$ and restricted it to the sensor position $y = u_{N-1}(t)$. The data were randomly disturbed with a noise level of $\delta = 5\%$, i.e., $\|y_\delta - y\|/\|y\| = 0.05$. A reconstruction by Algorithm 6.1
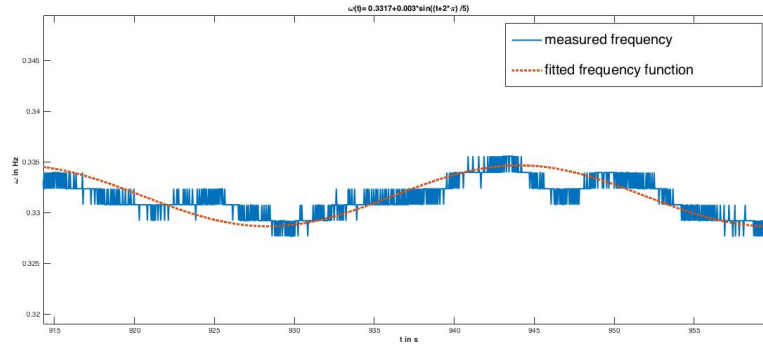
FIG. 6.2. *Frequency function from a GE 1.5 fitted with* $\omega(t) = 0.3317 + 0.003 \sin\left(\frac{t+2\pi}{5}\right)$.

with the exact data produced the exact imbalance. In case of disturbed data, the reconstructed imbalance was $253.2 \text{ kg} \cdot \text{m}$ at an angle of $27.5°$. The reconstruction error $\frac{\|p_{N-1}^0 - p_{rec}^0\|}{\|p_{N-1}^0\|}$ is 5%, which corresponds to the noise level. We remark that the error for the absolute value of the imbalance is only 1.3% while the error of the angle is 8.5%.

6.1.2. Disturbed constant frequency. A modern wind turbine operates with variable frequency. Even if the wind is strong enough to operate with nominal speed, the frequency usually changes a bit. A typical frequency function from a GE 1.5 wind turbine is shown in Figure 6.2. For our test, we assume that the frequency changes harmonically around a constant one like in the case displayed in Figure 6.2.

Setting. As in Section 6.1.1 we use the S77 wind turbine and the imbalance of $250 \text{ kg} \cdot \text{m}$ at $30°$. We assume that the frequency oscillates around the constant frequency $\omega_c = 0.64 \cdot \pi$; $\omega(t) = \omega_c + 0.05 \sin(\frac{\omega_c}{10} \cdot t)$. Assuming $\varphi(0) = 0$, we have

$$\varphi(t) = \omega_c t - \frac{0.5}{\omega_c} \cos\left(\frac{\omega_c}{10} \cdot t\right), \qquad \text{and}$$

$$\Omega(t) = \left[\omega^2(t) - i\, 0.005\, \omega_c \cos\left(\frac{\omega_c}{10} \cdot t\right)\right] e^{i\varphi(t)}.$$

A time interval of $[0; 5]$ s was chosen.

Vibration data. Artificial data can be produced via a forward computation of $u = T_n[p; \alpha; \beta]$, where α and β are the initial values taken from the constant frequency case. We can disturb the data randomly to simulate noise that would occur in real data. On the other hand, we can expect that the data from the constant frequency case are very close to the data of the disturbed frequency case as long as the disturbance of the frequency is small. Figure 6.3 displays the exact data for the constant frequency case compared to exact and randomly disturbed data produced with the forward model with variable frequency.

Reconstruction. The imbalance was reconstructed from the noisy data of the forward computation with T_n, where the data error level ranges from 5% to 25%. The absolute value $|p_{rec}^0|$ of the reconstructed imbalance, its relative error $E_{abs} = \frac{||p_{rec}^0| - |p_{N-1}^0||}{|p_{N-1}^0|}$, the angle φ_{N-1}^{rec}, its relative error $E_{angle} = \frac{|\varphi_{N-1}^{rec} - \varphi_{N-1}|}{|\varphi_{N-1}|}$, as well as the relative reconstruction error $E_p = \frac{\|p^0 - p_{rec}^0\|}{\|p^0\|}$ for each noise level are presented in Table 6.1. We also provide a reconstruction for data from the constant frequency model.
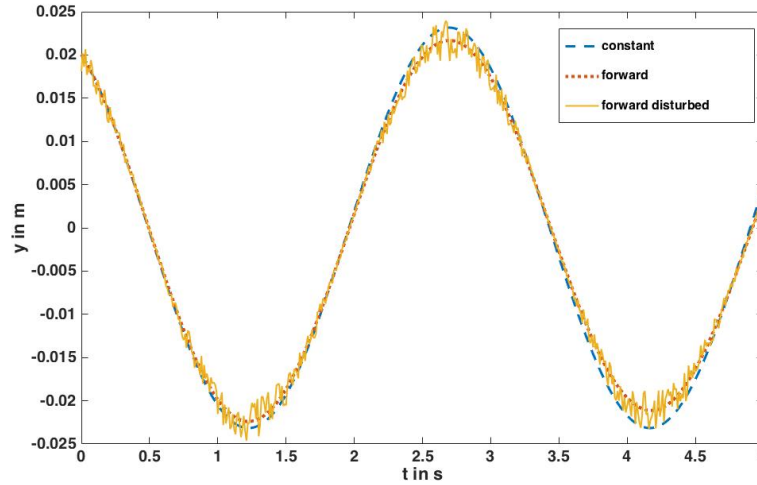
FIG. 6.3. *Data from the constant frequency case compared to exact and disturbed data produced with the forward operator T_n.*

TABLE 6.1
Reconstruction results for an S77 running with frequency $\omega(t) = \omega_c + 0.05 \sin(\omega_c \cdot t)$ for noisy data.

noise level	$|p^0_{rec}|$ in kgm	E_{abs}	φ^{rec}_{N-1} in °	E_{angle}	E_p
0%	250		30		
5%	252	1%	28.8	3.8 %	2.4%
10%	251.6	0.6%	28.7	4.3%	2.4%
15%	258	3%	28.9	3.5%	3.7%
20%	238	5%	26.6	11%	7.5%
25%	235	6%	43.6	45%	23%
constant	frequency	data			
0%	245	2%	41.4	38 %	20%

We observe that the reconstruction error is smaller than the noise level. Also, the reconstruction of the absolute value of the imbalance is more accurate than the reconstruction of the angle. For data from the constant frequency case, the absolute value of the reconstructed imbalance is still quite accurate while the angle shows a larger error.

6.1.3. Linear frequency.
Setting. The same setting as in the previous example was used with a linear frequency function. We assume a linear frequency growth from 0.28 Hz to 0.33 Hz in 5 s. Thus, $\omega(t) = 2\pi(0.01t + 0.28)$, $\varphi(t) = 0.01\pi t^2 + 0.56\pi$, and $\Omega(t) = \left[\omega^2(t) - i \, 0.02\pi\right] e^{i\varphi(t)}$.

Vibration data. The data were produced by a forward computation via $u = T_n[p; \alpha; \beta]$ and randomly disturbed noise with increasing noise level. To provide the initial values $\alpha = u(0)$ and $\beta = \dot{u}(0)$, we have computed u using the constant frequency approach with $\omega_c = 0.56\pi$, which corresponds to the initial frequency of 0.28 Hz. To simulate noisy measurements of the data, we

    a) added random noise to u with a noise level of 5–20%;

    b) assumed, in addition to the data error in u, an error in the function $\omega(t)$. Since ω is taken from measurements that are approximated by a linear function, we used a slightly different approximation to simulate that error: $\omega(t) = 2\pi(0.008t + 0.287)$

Reconstruction results. For both data a) and b) we get very stable results; cf. Table 6.2. The reconstruction error is much smaller than the data error. This indicates that the time variable approach is very suitable for the situation when measurements are taken during an idle-to-maximum run (e.g., for aircraft engines) or vice versa (e.g., for vacuum pumps).

TABLE 6.2
Reconstruction results for an S77 running with frequency $\omega(t) = \omega(t) = 2\pi(0.01t + 0.28)$ for noisy data.

noise level	$|p_{rec}^0|$ in kgm	E_{abs}	φ_{N-1}^{rec} in $^\circ$	E_{angle}	E_p
original	250		30		
a) 5%	249.7	0.15%	29.96	0.1 %	0.15%
10%	251	0.4%	29.86	0.46%	0.45%
15%	252	0.75%	30.3	1%	0.9%
20%	247.5	1%	30.03	0.1%	1%
b) disturbed	frequency	data			
20%	252	0.7%	30.5	1.8 %	1.2%

7. Summary and outlook. In this paper we have considered the inverse problem of reconstructing an imbalance distribution $\mathbf{p}^0$ in a rotating system from measured displacement data $\mathbf{u}(t)$ that are collected during a run of an rotating machinery with varying angular velocity $\omega(t)$. All restrictions posed by practical applications were taken into account. After discretization, our final algorithm uses a truncated SVD of the resulting system matrix to obtain a regularized solution. The method, tested with artificial data for different settings, provide stable results. In the cases where the frequency changes harmonically around a constant frequency or for a linear change of the frequency, the reconstruction error was at the same magnitude as the data error. Tests with real data from actual wind turbines or other rotating machinery remain a task for future work. In particular, the transformation of the usually measured acceleration/velocity data to the displacement data, which is the input for our algorithm, has to be considered.

Appendix A. Discretization of $\mathcal{K}_\Omega$. In this section we discretize equation (5.5) using a Galerkin scheme. Using (3.8) and (3.7), equation (5.5) reads

$$\sum_{i=1}^N \mathbf{e}_i \otimes z_i(t) = \sum_{i=1}^r \bar{\mathbf{B}}\mathbf{e}_i \otimes [\bar{p}_{L_i}^R (K\Omega^R)(t) - \bar{p}_{L_i}^I (K\Omega^I)(t)] + \sum_{i=1}^N \alpha_i \mathbf{e}_i \otimes 1 + \sum_{i=1}^N \beta_i \mathbf{e}_i \otimes t.$$

The functions $\Omega^R(t)$, $\Omega^I(t)$ are approximated in $L_{2,n}$ by

$$\sum_{j=1}^n \Omega_j^{R,I} \psi_j(t), \qquad \text{with} \quad (\Omega_j^{R,I})_{j=1}^n = \mathbf{D}^{-1} \left(\langle \psi_j, \Omega^{R,I} \rangle \right)_{j=1}^n,$$

and we define $\underline{\mathbf{c}} = (\langle \psi_j, 1 \rangle)_{j=1}^n$, $\underline{\mathbf{d}} = (\langle \psi_j, t \rangle)_{j=1}^n$ as in (5.4).

Here $\psi_j(t)$, $j = 1, \ldots, n$, are the basis functions of $L_{2,n}$. This implies that the tensor products $\{\mathbf{e}_i \otimes \psi_j\}_{i=1,\ldots,N}^{j=1,\ldots,n}$ form a basis of the finite-dimensional tensor subspace $\mathbb{R}^N \otimes L_{2,n} \subset \mathbb{R}^N \otimes L_2$. These basis functions serve as test functions in a Galerkin method. The equation above is transformed by computing the inner product on both sides with the test

IMBALANCE RECONSTRUCTION 447

functions. The left-hand side becomes

$$\left\langle \mathbf{e}_k \otimes \psi_\ell, \sum_{i=1}^N \mathbf{e}_i \otimes z_i \right\rangle = \sum_{i=1}^N \langle \mathbf{e}_k \otimes \psi_\ell, \mathbf{e}_i \otimes z_i \rangle = \sum_{i=1}^N \langle \mathbf{e}_k, \mathbf{e}_i \rangle \langle \psi_\ell, z_i \rangle$$

$$= \sum_{i=1}^N \delta_{ki} \langle \psi_\ell, z_i \rangle = \langle \psi_\ell, z_k \rangle .$$

The two last sums on the right-hand side become

$$\left\langle \mathbf{e}_k \otimes \psi_\ell, \sum_{i=1}^N \alpha_i \mathbf{e}_i \otimes 1 \right\rangle = \sum_{i=1}^N \alpha_i \langle \mathbf{e}_k, \mathbf{e}_i \rangle \langle \psi_\ell, 1 \rangle = \alpha_k \underline{\mathbf{c}}_l,$$

$$\left\langle \mathbf{e}_k \otimes \psi_\ell, \sum_{i=1}^N \beta_i \mathbf{e}_i \otimes t \right\rangle = \sum_{i=1}^N \beta_i \langle \mathbf{e}_k, \mathbf{e}_i \rangle \langle \psi_\ell, t \rangle = \beta_k \underline{\mathbf{d}}_l.$$

The first sum on the right-hand side becomes

$$\left\langle \mathbf{e}_k \otimes \psi_\ell, \sum_{i=1}^r \bar{\mathbf{B}} \mathbf{e}_i \otimes \sum_{j=1}^n [\bar{p}_{L_i}^R \Omega_j^R - \bar{p}_{L_i}^I \Omega_j^I](K\psi_j) \right\rangle$$

$$= \sum_{i=1}^r \langle \mathbf{e}_k, \bar{\mathbf{B}} \mathbf{e}_i \rangle \left\langle \psi_\ell, \sum_{j=1}^n [\bar{p}_{L_i}^R \Omega_j^R - \bar{p}_{L_i}^I \Omega_j^I](K\psi_j) \right\rangle$$

$$= \sum_{j=1}^n \langle \psi_\ell, (K\psi_j) \rangle \sum_{i=1}^r \langle \mathbf{e}_k, \bar{\mathbf{B}} \mathbf{e}_i \rangle \begin{bmatrix} \Omega_j^R & -\Omega_j^I \end{bmatrix} \begin{bmatrix} \bar{p}_{L_i}^R \\ \bar{p}_{L_i}^I \end{bmatrix} .$$

For all basis functions $\{\mathbf{e}_i \otimes \psi_j\}_{i=1,\dots,N}^{j=1,\dots,n}$, the above computations lead to a system of nN equations, which are combined in a vectorized set of equations

$$\begin{bmatrix} \langle \psi_1, z_1 \rangle \\ \vdots \\ \langle \psi_n, z_1 \rangle \\ \langle \psi_1, z_2 \rangle \\ \vdots \\ \langle \psi_n, z_2 \rangle \\ \vdots \\ \vdots \\ \langle \psi_1, z_N \rangle \\ \vdots \\ \langle \psi_n, z_N \rangle \end{bmatrix} = \sum_{j=1}^n \begin{bmatrix} \langle \psi_1, K\psi_j \rangle \sum_{i=1}^r \bar{b}_{1i}(\mathbf{\Omega}p)_j^{(i)} \\ \vdots \\ \langle \psi_n, K\psi_j \rangle \sum_{i=1}^r \bar{b}_{1i}(\mathbf{\Omega}p)_j^{(i)} \\ \langle \psi_1, K\psi_j \rangle \sum_{i=1}^r \bar{b}_{2i}(\mathbf{\Omega}p)_j^{(i)} \\ \vdots \\ \langle \psi_n, K\psi_j \rangle \sum_{i=1}^r \bar{b}_{2i}(\mathbf{\Omega}p)_j^{(i)} \\ \vdots \\ \vdots \\ \langle \psi_1, K\psi_j \rangle \sum_{i=1}^r \bar{b}_{Ni}(\mathbf{\Omega}p)_j^{(i)} \\ \vdots \\ \langle \psi_n, K\psi_j \rangle \sum_{i=1}^r \bar{b}_{Ni}(\mathbf{\Omega}p)_j^{(i)} \end{bmatrix} + \begin{bmatrix} \alpha_1 \underline{\mathbf{c}} \\ \vdots \\ \alpha_N \underline{\mathbf{c}} \end{bmatrix} + \begin{bmatrix} \beta_1 \underline{\mathbf{d}} \\ \vdots \\ \beta_N \underline{\mathbf{d}} \end{bmatrix},$$

where

$$(\mathbf{\Omega}p)_j^{(i)} = \begin{bmatrix} \Omega_j^R & -\Omega_j^I \end{bmatrix} \begin{bmatrix} \bar{p}_{L_i}^R \\ \bar{p}_{L_i}^I \end{bmatrix} .$$

In terms of Kronecker products, with $\mathbf{z}_i = (\langle \psi_j, z_i \rangle)_{j=1}^n$, this is the same as

$$\sum_{i=1}^{N} \mathbf{e}_i \otimes \mathbf{z}_i = (\bar{\mathbf{B}} \otimes \mathbf{F})(\mathbf{I}_r \otimes \mathbf{\Omega}) \sum_{i=1}^{r} \mathbf{e}_i \otimes \begin{bmatrix} \bar{p}_{L_i}^R \\ \bar{p}_{L_i}^I \end{bmatrix} + (\mathbf{I}_{\mathbb{R}^N} \otimes \underline{\mathbf{c}})\alpha + (\mathbf{I}_{\mathbb{R}^N} \otimes \underline{\mathbf{d}})\beta,$$

and thus (5.6) follows.

REFERENCES

[1] H. BRAKHAGE, *On ill-posed problems and the method of conjugate gradients*, in Inverse and Ill-Posed Problems, H. Engl and C. Groetsch, eds., Notes Rep. Math. Sci. Engrg. Vol. 4, Academic Press, Boston, 1987, pp. 165–175.

[2] M. DEFRIESE AND C. DE MOL, *A note on stopping rules for iterativ regularization methods and filtered svd*, in Inverse Problems: An Interdisciplinary Study, P. Sabatier, ed., Adv. Electron. Electron Phys., Suppl. 19, Academic Press, London, 1987, pp. 261–268.

[3] V. DICKEN, I. MENZ, P. MAASS, J. NIEBSCH, AND R. RAMLAU, *Nonlinear inverse unbalance reconstruction in rotor dynamics*, Inverse Probl. Sci. Eng., 13 (2005), pp. 507–543.

[4] H. W. ENGL, M. HANKE, AND A. NEUBAUER, *Regularization of Inverse Problems*, Kluwer, Dordrecht, 1996.

[5] H. W. ENGL AND R. RAMLAU, *Regularization of inverse problems*, in Encyclopedia of Applied and Computational Mathematics, B. Engquist, ed., Springer, Berlin, 2015, pp. 1233–1241.

[6] R. GASCH AND K. KNOTHE, *Strukturdynamik 2*, Springer, Berlin, 1989.

[7] C. W. GROETSCH, *The Theory of Tikhonov Regularization for Fredholm Equations of the First Kind*, Pitman, Boston, 1984.

[8] Z. HAMEED, Y. S. HONG, Y. M. CHO, S. H. AHN, AND C.-K. SONG, *Condition monitoring and fault detection of wind turbines and related algorithms: A review*, Renewable and Sustainable Energy Reviews, 13 (2009), pp. 1–39.

[9] M. HANKE, *Conjugate Gradient Type Methods for Ill-posed Problems*, Longman Scientific & Technical, Harlow, 1995.

[10] P. C. HANSEN, *Truncated singular value decomposition solutions to discrete ill-posed problems with ill-determined numerical rank*, SIAM J. Sci. Statist. Comput., 11 (1990), pp. 503–518.

[11] ———, *Analysis of discrete ill-posed problems by means of the L-curve*, SIAM Rev., 34 (1992), pp. 561–580.

[12] P. C. HANSEN AND D. P. O'LEARY, *The use of the L-curve in the regularization of discrete ill-posed problems*, SIAM J. Sci. Comput., 14 (1993), pp. 1487–1503.

[13] P. C. HANSEN, T. SEKII, AND H. SHIBAHASHI, *The modified truncated SVD method for regularization in general form*, SIAM J. Sci. Statist. Comput., 13 (1992), pp. 1142–1150.

[14] M. HESTENES AND E. STIEFEL, *Methods of conjugate gradients for solving linear systems*, J. Research Nat. Bur. Standards, 49 (1952), pp. 409–436.

[15] J. KAIPIO AND E. SOMERSALO, *Statistical and Computational Inverse Problems*, Springer, New York, 2005.

[16] S. KINDERMANN, *Convergence analysis of minimization-based noise level-free parameter choice rules for linear ill-posed problems*, Electron. Trans. Numer. Anal., 38 (2011), pp. 233–257.
http://etna.ricam.oeaw.ac.at/vol.38.2011/pp233-257.dir/pp233-257.pdf

[17] S. KINDERMANN, *Discretization independent convergence rates for noise level-free parameter choice rules in the regularization of ill-conditioned problems*, Electron. Trans. Numer. Anal., 40 (2013), pp. 58–81.
http://etna.ricam.oeaw.ac.at/vol.40.2013/pp58-81.dir/pp58-81.pdf

[18] S. KINDERMANN AND A. NEUBAUER, *On the convergence of the quasioptimality criterion for (iterated) Tikhonov regularization*, Inverse Probl. Imaging, 2 (2008), pp. 291–299.

[19] A. KIRSCH, *An Introduction to the Mathematical Theory of Inverse Problems*, 2nd ed., Springer, New York, 2011.

[20] L. LANDWEBER, *An iteration formula for Fredholm integral equations of the first kind*, Amer. J. Math., 73 (1951), pp. 615–624.

[21] A. K. LOUIS, *Convergence of the conjugate gradient method for compact operators*, in Inverse and Ill-Posed Problems, H. Engl and C. Groetsch, eds., Notes Rep. Math. Sci. Engrg. Vol. 4, Academic Press, Boston, 1987, pp. 177–183.

[22] A. K. LOUIS, *Inverse und Schlecht Gestellte Probleme*, Teubner, Stuttgart, 1989.

[23] V. A. MOROZOV, *Methods for Solving Incorrectly Posed Problems*, Springer, New York, 1984.

[24] J. NIEBSCH AND R. RAMLAU, *Mathematical imbalance determination from vibrational measurements and industrial applications*, in ASME 2008 Proceedings of IDETC/CIE, vol. 3, ASME, New York, 2008, pp. 1035–1042.

[25] ———, *Imbalance estimation without test masses for wind turbines*, J. Sol. Energy Eng., 131 (2009), Art. 0111010 (7 pages).

[26] J. NIEBSCH, R. RAMLAU, AND K. M. SOODHALTER, *Solution of coupled differential equations arising from imbalance problems*, Electron. Trans. Numer. Anal., 46 (2017), pp. 89–106.
http://etna.ricam.oeaw.ac.at/vol.46.2017/pp89-106.dir/pp89-106.pdf

[27] A. TIKHONOV, *Regularization of incorrectly posed problems*, Soviet Math. Dokl., 4 (1963), pp. 1624–1627.

[28] ———, *Solution of incorrectly formulated problems and the regularization method*, Soviet Math. Dokl., 4 (1963), pp. 1035–1038.

[29] C. R. VOGEL, *Computational Methods for Inverse Problems*, SIAM, Philadelphia, 2002.

[30] S. ZHOU AND J. SHI, *Active balancing and bibration control of rotating machinery: a survey*, The Shock and Vibration Digest, 33 (2001), pp. 361–371.